
Of arcs and vaults: the biomechanics of bone-cracking in spotted hyenas (*Crocuta crocuta*)

JAIME B. TANNER^{1*}, ELIZABETH R. DUMONT⁴, SHARLEEN T. SAKAI²,
BARBARA L. LUNDRIGAN^{1,3} and KAY E. HOLEKAMP^{1,3}

Departments of ¹Zoology and ²Psychology, ³Michigan State University Museum, Michigan State University, East Lansing, MI 48824, USA

⁴Department of Biology, University of Massachusetts at Amherst, Amherst, MA 01003, USA

Received 11 September 2007; accepted for publication 2 January 2008

The ability to break open large bones has evolved independently in only three groups of carnivorous mammals, all of which have robust teeth, vaulted foreheads, and pronounced sagittal crests. One unusual skull feature, present in bone-cracking members of the family Hyaenidae, is a caudally elongated frontal sinus, hypothesized to function in resistance to bending and stress dissipation during bone-cracking. In the present study, we used finite element (FE) analysis to examine patterns of stress distribution in the spotted hyena (*Crocuta crocuta*) skull during unilateral biting, and inquire about the functional role of the fronto-parietal sinus in stress dissipation. We constructed and compared three FE models: (1) a 'normal' model of an adult *Crocuta* skull; (2) a model in which the caudal portion of the fronto-parietal sinus was filled with bone; and (3) a model in which we flattened the sagittal crest to resemble the plate-like crests of other mammals. During biting, an arc of stress extends from the bite point up through the vaulted forehead and along the sagittal crest. Our results suggest that pneumatization of the hyena's skull both enhances its ability to resist bending and, together with the vaulted forehead, plays a critical role in evenly dissipating stress away from the facial region. © 2008 The Linnean Society of London, *Biological Journal of the Linnean Society*, 2008, **95**, 246–255.

ADDITIONAL KEYWORDS: durophagy – feeding – finite-element analysis – fronto-parietal sinus – skull morphology.

INTRODUCTION

Organisms that cope with extreme challenges in their environment provide excellent opportunities for exploring the relationship between form and function (Wainwright & Reilly, 1994). The skulls of carnivores are especially interesting in this context because they allow us to examine the interplay between forces shaping the highly developed neural and sensory organs critical for locating and capturing prey, and those shaping a feeding apparatus designed for both the capture of uncooperative prey and the processing

of their carcasses. The skulls of bone-cracking animals represent extreme examples and they possess a suite of cranio-dental characteristics that maximize their ability to feed on virtually all components of a carcass.

Although extant carnivores provide useful models for the study of skull form and function, *in vivo* studies of the forces and strains generated during biting are often logistically and practically impossible to accomplish. Only scant data are available documenting bite forces generated by carnivores, and almost all of these are from captive animals (Dessem, 1989; Binder & Van Valkenburgh, 2000). Captive studies yield bite force maxima that almost certainly underestimate the true feeding capabilities of these animals in the wild, likely due to differences in diet, and often a lack of competition for food (Stefen, 1997).

*Corresponding author. Current address: Department of Biology, University of Massachusetts at Amherst, 221 Morrill Science Center 3, Amherst, MA 01003
E-mail: tannerja@msu.edu

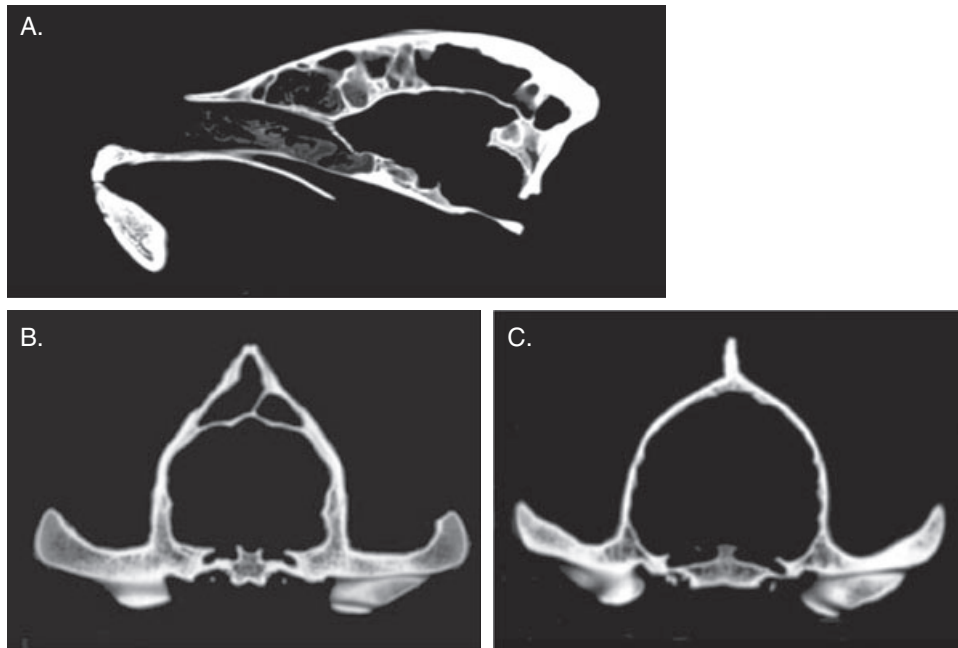


Figure 1. Computed tomography slices of sagittal (A) and coronal (B) views of a *Crocuta* skull showing the pneumatized sagittal crest, and (C) a coronal view of a wolf (*Canis lupis*) showing the more typical plate-like sagittal crest found in nonhyaenid mammals.

Such limitations force us to look elsewhere for methods to more accurately assess the relationship between form and function in carnivore skulls. In the present study, we used finite element (FE) analysis to evaluate this relationship in the skulls of spotted hyenas (*Crocuta crocuta*).

Spotted hyenas are highly durophagous animals that are capable of breaking open and consuming bones of large diameter. These gregarious carnivores are recently descended from carrion-feeding ancestors (Lewis & Werdelin, 2000; Koepfli *et al.*, 2006). Bone-cracking forms have appeared only a few times in the evolutionary history of carnivorans: among hyaenids, percrocotids, and borophagine canids, with only hyaenids surviving to the present. Comparative analysis reveals some striking morphological similarities among the various bone-cracking forms including large body size, a simplified but robust dentition, a complex multidimensional structure in the tooth enamel, modified dentary bones, and a vaulted forehead (Biknevicius & Ruff, 1992; Biknevicius & Van Valkenburgh, 1996; Stefen, 1997; Rensberger, 1999; Rensberger & Wang, 2005; Therrien, 2005; Van Valkenburgh, 2007). Additionally, these bone-cracking carnivores typically have larger jaw muscles than their nondurophagous relatives and, consequently, larger muscle attachment area such as a prominent sagittal crest and wide bi-zygomatic breadth (Werdelin, 1989). Bone-cracking hyaenids and borophagine

canids have uniquely vaulted foreheads created by an enlarged frontal sinus. Based on the work of Buckland-Wright (1971, 1978), which suggested that compressive forces travel in an arc from the bite point dorsally through the region anterior to the eye orbit, Werdelin (1989) hypothesized that this vaulting creates an arc of bone that transfers stresses incurred during biting from the facial region caudally along the sagittal crest.

Although this suite of adaptations for durophagy occurs in all bone-cracking carnivores, only extinct and extant bone-cracking members of the Family Hyaenidae possess a caudally-elongated frontal sinus that invades the parietal bones and completely overlies the braincase (Paulli, 1900; Negus, 1958; Buckland-Wright, 1969; Joeckel, 1998). Thus, the skull is not only pneumatized anteriorly between the postorbital processes (as in borophagines), but also all along the sagittal crest (Fig. 1A). The presence of the elongated fronto-parietal sinus within the sagittal crest of bone-cracking hyenas results in the unique triangular cross section (Fig. 1B), which is dramatically different from the laterally compressed, plate-like sagittal crest of other mammals (Fig. 1C). Interestingly, the only other carnivore known to have a highly specialized and enlarged fronto-parietal sinus is the giant panda (*Ailuropoda melanoleuca*), which is also durophagous (Davis, 1964; Jin *et al.*, 2007).

In his descriptive study of the elongated fronto-parietal sinus, Joeckel (1998) likened the space created by the caudal portion of the sinus to an architectural shell or arch, and suggested that the sinus increases structural support by enhancing resistance to muscular loads applied to the sagittal crest during bone cracking. Based on principles derived from structural engineering, he predicted that the pneumatized sagittal crest in hyenas should be more resistant to bending stress and vertical loading by the temporalis muscles than the plate-like sagittal crests of other mammals. Although these are interesting ideas, the relative importance of the elongated fronto-parietal sinus in strengthening and lightening the skull remains unclear. For example, it is possible that it is the expanded base of the crest, rather than the fact that the crest is hollow that makes it more resistant to large muscle forces during biting. In the present study, we used the FE method to predict patterns of stress distribution in an adult *Crocuta* skull during a bone-cracking bite and test Joeckel's hypothesis about the role of the fronto-parietal sinus in bending resistance of the sagittal crest. We also evaluated more broadly the function of the sinus in the context of stresses generated by both muscle loading and bite forces.

We built and compared three different FE models: (1) a detailed model of the skull of an adult female spotted hyena; (2) a model of the same specimen in which the parietal portion of the pneumatized fronto-parietal sinus was filled in with bone; and (3) a third model in which we modified and flattened the sagittal crest so that it resembled the more plate-like crests of other mammals. If Joeckel's hypothesis is correct (i.e. the elongated fronto-parietal sinus functions to resist bending of the sagittal crest), then the model with the normal sagittal crest should be less stressed during biting than the model with the flattened crest. If the function of the sinus is purely to lighten the skull, then normal and 'filled' models should undergo similar stress regimes. Because the FE method allows us to experimentally manipulate morphology and visualize the effects of these manipulations on mechanical performance, we can use it to evaluate the influence of competing demands for bite force, bone strength, and skull mass in the evolution of skull form among these durophagous carnivores.

MATERIAL AND METHODS

The three FE models used in this study were all based on the skull of one 55-month-old adult female *Crocuta crocuta* (Michigan State University Museum; MSU 36567). This specimen originated from a longitudinal study population of free-living spotted hyenas in the Masai Mara National Reserve in southwestern

Kenya (Frank, Holekamp & Smale, 1995). The specimen was scanned on a General Electric Discovery ST 16 slice scanner at the Department of Radiology at Michigan State University, with a slice thickness of 0.625 mm. Methods for generating a 3D FE model from computed tomography scans follow Dumont, Piccirillo & Grosse (2005). Cranial sutures of adult hyenas are completely fused (Schweikher, 1930) and therefore were not included in the model.

We used Geomagic Studio (Raindrop Geomagic Inc.) to alter the surface model based on the scans (the 'normal' model; Fig. 2A) to create the two modified morphologies. For the 'filled' model (Fig. 2B), the sinus cavity was truncated at the post-orbital processes; the anterior portion of the fronto-parietal sinus and the external morphology of the sagittal crest were not altered in any way. For the 'flattened' model (Fig. 2C), we again removed the sinus cavity caudal to the post-orbital processes and also flattened the crest to form a thin blade-like crest that was similar in shape to those found in other crest-bearing mammals (Fig. 1C). All three surface models ('normal', 'filled', and 'flattened') were saved from Geomagic as STL files and then imported to the FE analysis tool Strand7 (Strand7 Pty Ltd.). We used the solid mesh generation algorithm in Strand7 to create a volumetric mesh composed of four-noded tetrahedra from each surface model. Despite their morphological differences, the resulting FE models were similar in size ('normal' model = 1 319 307 elements, 'filled' model = 1 332 181 elements, 'flattened' model = 1 255 253 elements).

Unfortunately, there are no data available summarizing Young's modulus or Poisson's ratio values for bone in hyena skulls. Therefore, we assigned our models values for the material properties of cortical bone used by Verrue, Dermaut & Verheghe (2001) for FE models of dog skulls ($E = 1.37 \times 10^4$ MPa; $\nu = 0.3$). We modeled bone as homogeneous and isotropic, even though this is not likely to be the case (Currey, 2002). Therefore, the absolute values of stress predicted by our model may not reflect actual values, and should be interpreted with caution. Past studies have shown that, although varying elastic properties may cause slight variations in the magnitude of stress, overall gross patterns of stress distribution are quite robust (Strait *et al.*, 2005). Because we applied the same material properties to each of our models, we can confidently compare stress distributions among the three models, and attribute any differences observed to modifications in the morphology of the sagittal crest.

We applied loads to our models that mimic the forces produced by the three main jaw-adductor muscles: temporalis, masseter, and pterygoid. Data summarizing the average mass of unilateral

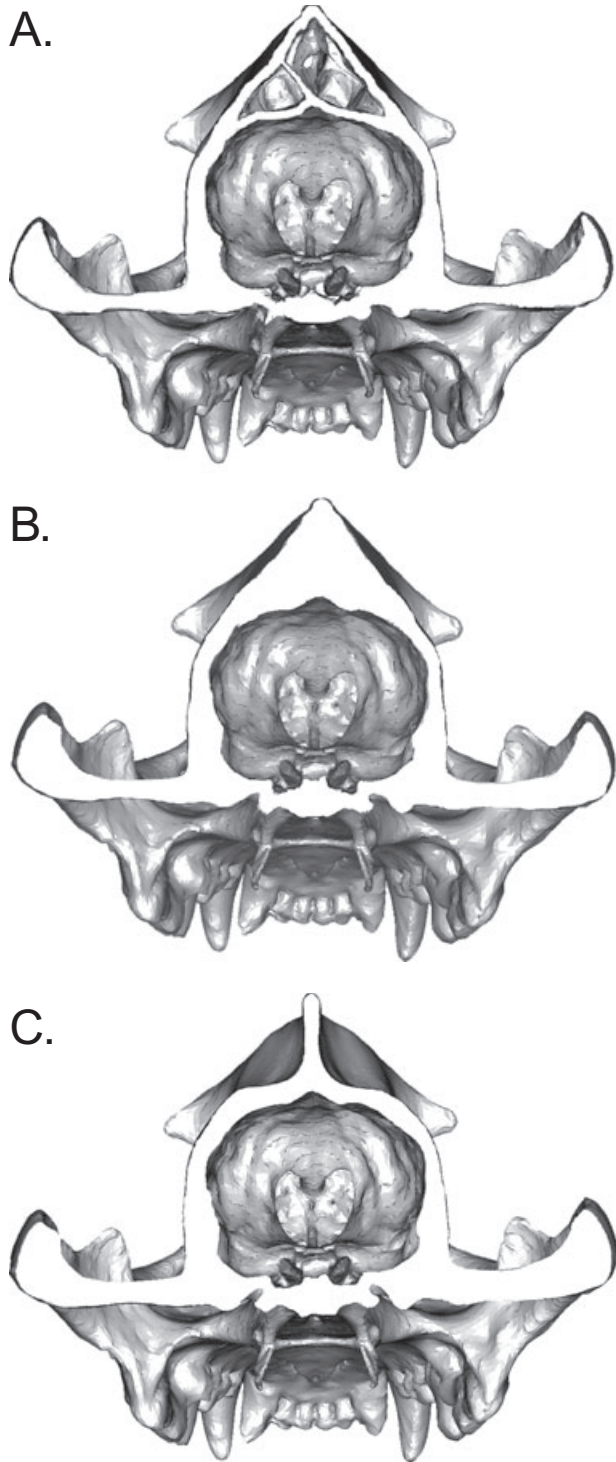


Figure 2. Comparison of STL surface representations with a posterior coronal cross-section illustrating the different morphologies of the (A) normal, (B) filled, and (C) flattened models.

temporalis and masseter muscles ($\bar{x} = 247 \pm 18.2$ g and $\bar{x} = 136 \pm 9.3$ g, respectively) were drawn from four necropsies of *Crocuta* conducted in the field (J.B.T.). Based on the relative size of the pterygoids in hyenas, and on data from felids (Gorniak & Gans, 1980), we estimated that the pterygoids contribute approximately 18% to the total mass of the jaw adductors. Therefore, we modeled the relative contribution of temporalis : masseter : pterygoid to adductor muscle force production as 50 : 32 : 18. The areas of attachment for each of the three muscle groups were based on descriptions of *Crocuta* and *Hyaena* myological studies by Buckland-Wright (1969) and also from our own field necropsies. To define the vectors of muscle force, we identified a node on the mandible within the region of attachment of each muscle. As in previous studies (Strait *et al.*, 2005), we constrained the models at one node on each articular surface of the temporomandibular joint. These constraints defined an axis around which the models could rotate in response to muscle forces. A node on the occlusal surface of the third premolar was also constrained in order to generate a reaction force that models bite force. Hyenas, like other carnivores, use unilateral biting during feeding (Biknevicius & Van Valkenburgh, 1996), and therefore we loaded our model to reflect forces incurred by one side of the jaw.

After defining muscle attachment sites and constraints, we used the Visual Basic program BONELOAD to apply muscle forces to FE models (Grosse *et al.*, 2007). This loading algorithm applies muscle forces based on both the traction that muscles generate and the normal forces that accumulate as muscle fibers wrap around curved bone surfaces. For each FE model, an initial analysis was run using an arbitrary total muscle force. Based on the resulting bite reaction force (measured perpendicular to the palate at the constrained premolar), we then adjusted the muscle loads to obtain a biologically relevant bite force. In captivity, measures of bite forces up to 3500 N have been obtained from spotted hyenas (Binder & Van Valkenburgh, 2000). However, Stefen (1997) and others (Erickson *et al.*, 1996; Meers, 2002; Therrien, 2005) estimate that 7000–9000 N are required to crack open the long bones of ungulates, on which wild hyenas commonly feed. Therefore we applied muscle loads to each FE model here to generate a conservative bite force of 5500 N. However, it is important to point out that, because these FE analyses were linear, identical patterns of stress distribution are generated no matter what magnitude of bite force is used. Moreover, ultimate failure of the models under extremely high loads is predicted by the location and magnitude of maximum stress at any bite force value.

The resulting FE analyses were compared in two ways. First, we visually inspected the results to compare and contrast the magnitude and distribution of von Mises stress, a predictor of failure for ductile materials due to distortion or shear. These are referred to as our 'qualitative' results. Second, we constructed histograms to compare the distribution of stress within two separate regions of the skull: the face and the cranial vault. The face included the entire skull anterior to the post-orbital processes, and the vault included the lateral and posterior walls of the braincase and the sagittal crest. Third, we compared the absolute muscle forces required to generate 5500 N of bite force in each model. The histograms and muscle forces are referred to as our 'quantitative' results.

RESULTS

The patterns of stress distribution in the normal adult *Crocota* model during unilateral right-sided biting are illustrated in Figure 3A. When sufficient muscle loads were applied to generate 5500 N of bite force, high areas of stress appeared on the working side maxilla anterior to the orbit and dorsal to the infraorbital foramen. Additionally, there was a hotspot of stress just anterior to the jugal-squamosal suture in the zygomatic arch. As predicted by Buckland-Wright (1971, 1978) and Werdelin (1989), an arc of stress extended from the bite point through the region anterior to the orbit, and along the vaulted forehead. This arc of stress then gradually dissipated posteriorly along the sagittal crest. The anterior portion of the braincase experienced somewhat higher concentrations of stress than did the rest of the braincase. Stress along the crest was distributed around the external surface of the fronto-parietal sinus and along the trabeculae within it (Fig. 4A).

Both the filled and flattened models deviated from the patterns observed in the normal model. Overall, the filled model experienced less stress than that observed in the normal model (Fig. 3B). As in the normal model, an arc of stress extended from the bite point to the vaulted forehead; however, the stress pathway terminated just posterior to the postorbital processes. Therefore, the sagittal crest and braincase were less stressed than in the normal model (Fig. 4B). The filled model exhibited higher concentrations of localized stress on the working side of the vaulted forehead (illustrated by the yellow area of stress adjacent to the postorbital process on the working side), and on the anterior edge of the orbit, compared with the other two models.

The flattened model exhibited by far the greatest stress values along the sagittal crest, as well as slightly elevated stress in the anterior portion of the

braincase (Fig. 3C). There are high values of stress throughout the crest but the highest stress values are in the dorsal region, as indicated in a coronal cross-section (Fig. 4C). Stresses on the working side maxilla were also higher than in the other two models.

Only slight differences were observed among the three models with respect to the amount of localized stress in the facial region, with the flattened model showing the highest stress values in this area. The most obvious differences among the models were seen in the area between the post-orbital processes and along the sagittal crest. The flow of stress from the face to the sagittal crest evident in the normal and flattened models was interrupted in the filled model. The normal model, although more heavily stressed than the filled model, illustrated an intermediate pattern of stress distribution compared with the other two models. The stresses incurred during unilateral biting appeared to be more evenly distributed in the normal model than in either of the other models, with lower stresses on the edge of the orbit and in the forehead than in the filled model, as well as lower stresses along the sagittal crest and zygomatic arch than in the flattened model.

Quantitative differences among the three models in the percent of total skull volume stressed in the face and cranial vault mirrored the results of the qualitative comparisons (Fig. 5). For the cranial vault, the filled model was clearly the least stressed, and the flattened model the most stressed. Although variation in the proportion of the facial skeleton experiencing stress was very slight, the areas that were most highly stressed differed among the three models. The filled model had higher concentrations of stress along the edge of the orbit and on the forehead than did the other two models, whereas the flattened model had higher values in the maxilla.

Considering these results, it is important to point out that the muscle forces required to produce 5500 N of bite force differed among the three models (Table 1). The filled model required the least amount of muscle force, whereas the flattened model required the greatest amount of force to produce the same bite force; the normal model was intermediate. From a slightly different perspective, the muscle forces required to produce 5500 N of bite force in the normal model produced a bite force of 5750 N in the filled model and a bite force of 5350 N in the flattened model. Thus, the normal model was intermediate in terms of the efficiency of transferring muscle forces to bite force, and the filled model was most efficient.

DISCUSSION

In the present study, the FE method allowed us to experiment with alternative morphologies and take a

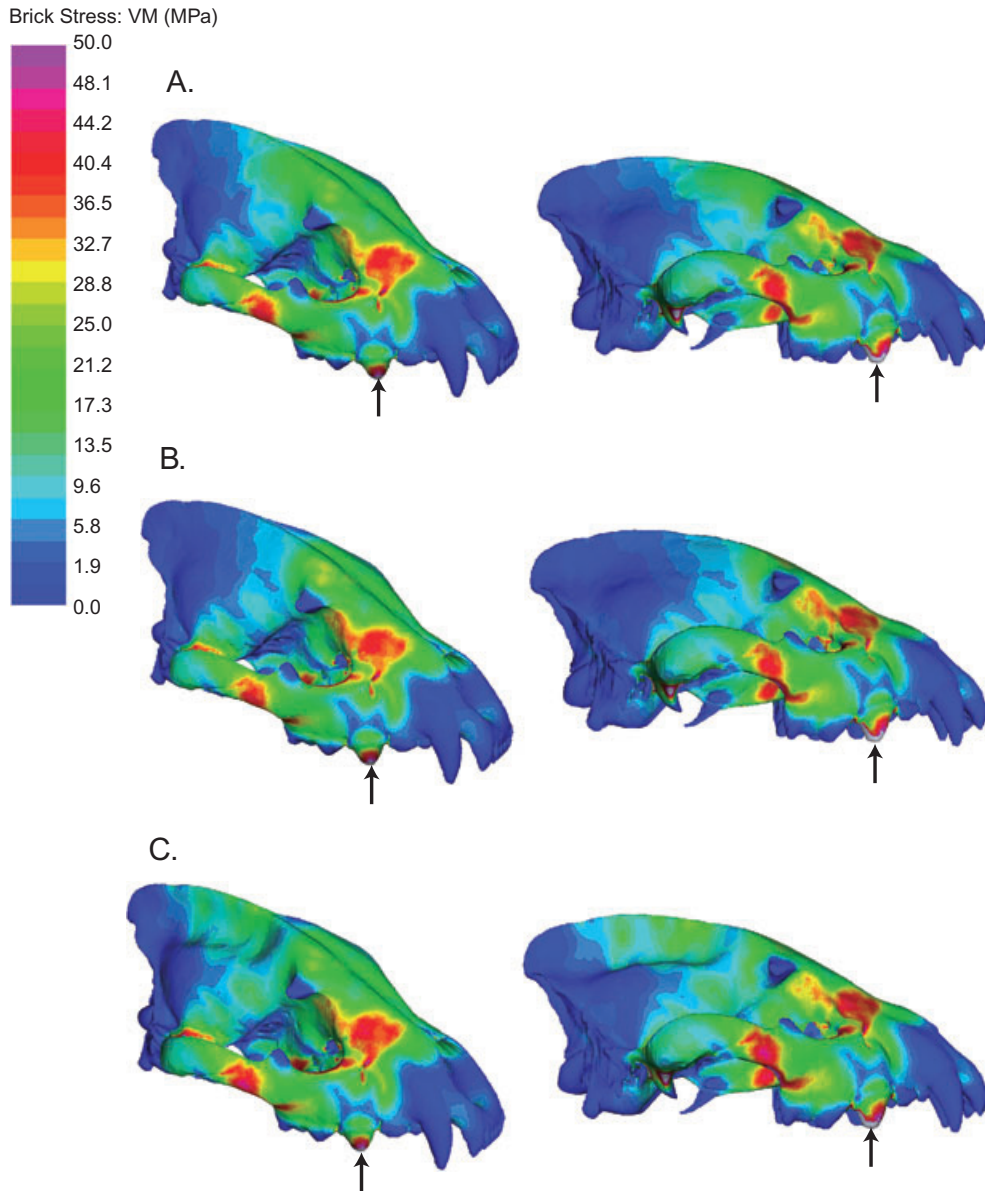


Figure 3. Von Mises stress during unilateral right-side biting in the three-quarter lateral view (left) and the lateral view (right) for the (A) normal, (B) filled, and (C) flattened models. Stress is measured in megapascals (MPa) with warmer colours representing higher stress. Arrows indicate the bite point on the third premolar in each model.

holistic approach to predicting patterns of force distribution during biting behavior. This kind of detailed 'snapshot' of the stress state throughout the entire skull is impossible to achieve using any other technique, and highlights the utility of this method in comparative biology, especially when investigating areas of the skull, such as the elongated fronto-parietal sinus, from which it would otherwise be impossible to collect data (Ross, 2005). This study illustrates the usefulness of the FE method in hypothesis-testing, and its potential for addressing

questions about form-function relationships in organisms that cope with extreme conditions.

Given the unique challenges of a highly durophagous diet and the unique morphology observed in the feeding apparatus of the hyena, the present study provides compelling evidence that the form of the fronto-parietal sinus, and consequently the pneumatized sagittal crest, allows hyenas to cope effectively with the large forces experienced during bone-cracking. Of the three morphologies investigated, the pneumatized sagittal crest is the most efficient at

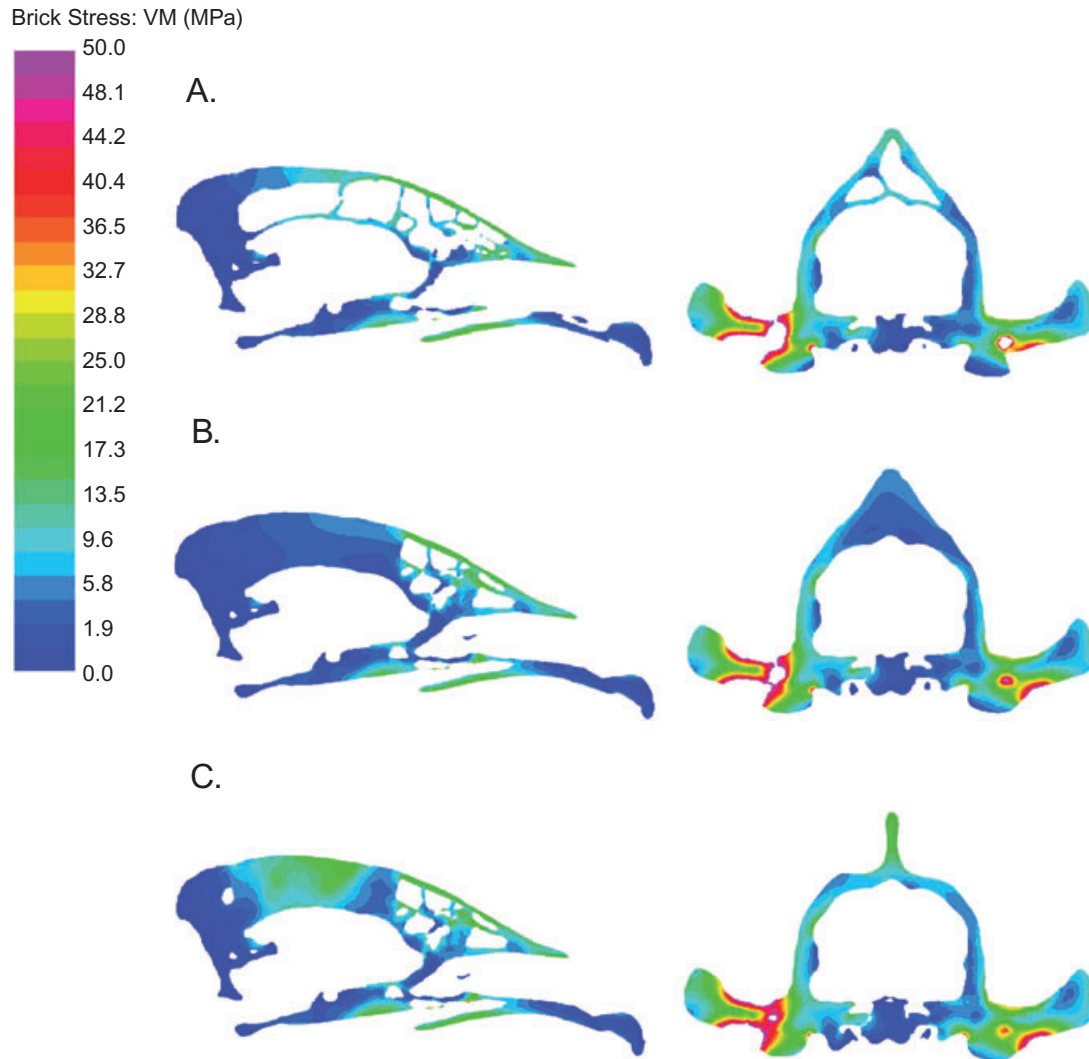


Figure 4. Sagittal (left) and coronal (right) slices showing Von Mises stress distribution (in MPa) in the sagittal crests of the (A) normal, (B) filled, and (C) flattened models. Note the distribution of stress to the trabeculae within the fronto-parietal sinus as well as along the other bones. The warm colours and white areas on the left temporomandibular joint illustrate the large stresses on the contralateral jaw joint during unilateral right-side biting.

meeting the concurrent demands of the massive jaw musculature necessary for generating large bite forces, and skull strength sufficient for resisting large stresses, without increasing skull weight.

The general pattern of stress distribution observed in our normal model conforms to predictions made by Buckland-Wright (1971, 1978) and Werdelin (1989), who concluded that forces generated in hyenas during premolar biting must pass through the face anterior to the orbit, and then continue along the vaulted forehead to the sagittal crest. The greater stress in the sagittal crest of the flattened model than in the normal model also supports the hypothesis by Joeckel (1998) that the elongated fronto-parietal sinus helps to resist loads by dissi-

pating stress along its curvature (Figs 3, 4). Specifically, the stresses are dissipated laterally along the edges of the sinus (Fig. 4A) as well as caudally (Fig. 3A). However, although Joeckel predicted that the highest areas of stress in a plate-like crest would be found at the base, our flattened model revealed higher stress along the top of the crest (Fig. 4C). This may be due to the tensile stresses caused by the simultaneous pull of the muscles on either side of the plate-like crest in our FE model. If temporalis activity were asymmetrical, as is probable during the early phase of biting, it is likely that there would indeed be bending stress at the base of the crest. However, in the present study, we analyzed the symmetrical muscle loads that typically accompany peak

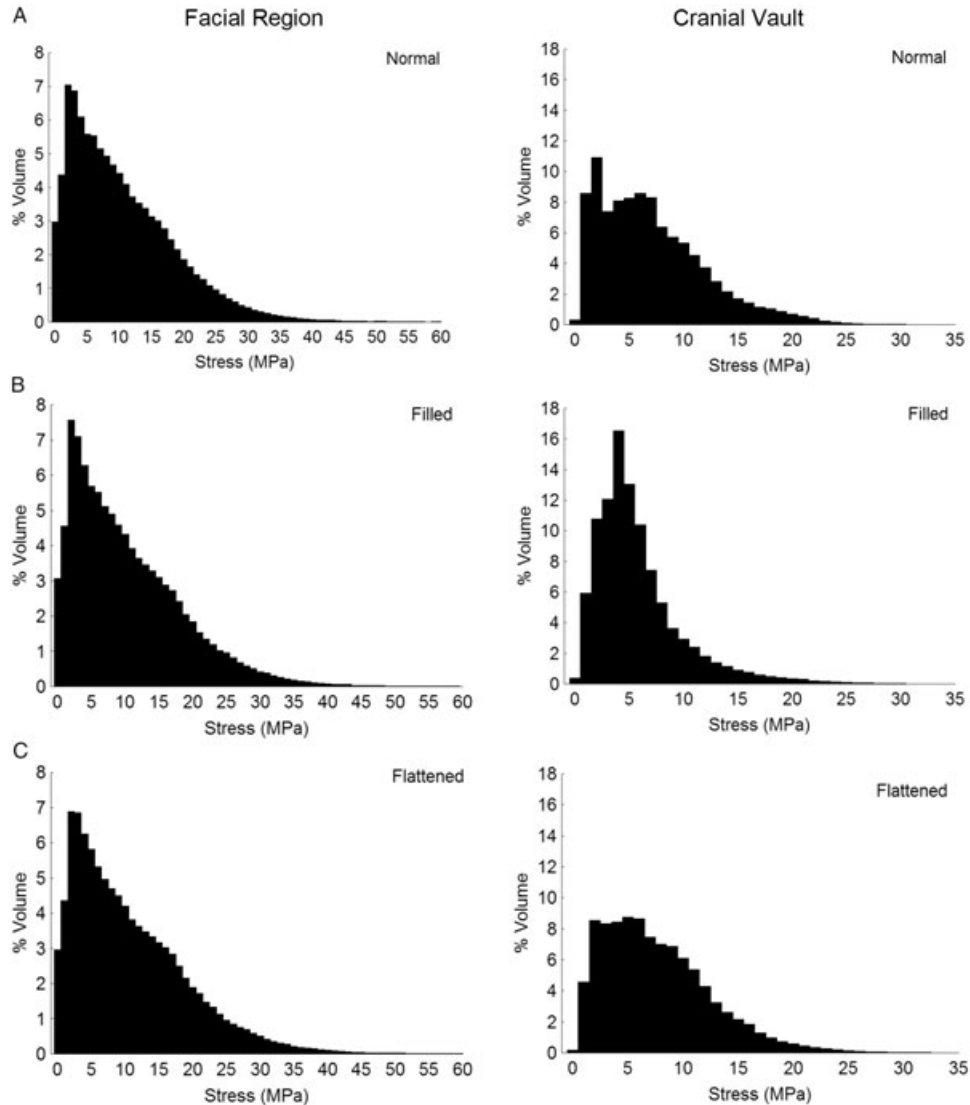


Figure 5. The percent of total volume of the facial region (left) and cranial vault (right) stressed (in MPa) during biting in (A) normal, (B) filled, and (C) flattened models. The area under the curve represent 98–99% of the volumes of the cranial vault and facial region, respectively.

Table 1. Muscle forces applied to each model in order to produce 5500 N of bite force

Model	Temporalis (N)	Masseter (N)	Pterygoid (N)	Total (N)
Normal	101.6	64.6	45.2	211.4
Filled	97.2	61.8	43.2	202.2
Flattened	104.5	66.4	46.5	217.4

Values represent the sum of identical forces applied on the left and right.

bite force (Hylander, Ravosa & Ross, 2004). In any case, Joeckel (1998) was correct in his interpretation that the vaulted sagittal crest provides more structural support during biting than does a flattened

crest. Certainly, the greatest variation in stress among our three models occurred in the cranial vault. It is noteworthy that, despite the limited technology available to earlier researchers, their insights

into these unique adaptations have proven to be remarkably accurate.

Including the filled model in our analysis allowed us to extend the work of Joeckel (1998) by teasing apart the relative importance of the fronto-parietal sinus in resisting muscle loads versus lightening the skull. The volume of the fronto-parietal sinus in this specimen is 89.7 cm³ (ST Sakai, unpubl. data). Assuming the density of bone is similar to that found in primate and canid skulls (approximately 1.62 g cm⁻³) (Novacosky & Popkin, 2005; Wang, Strait & Dechow, 2006), our filled model would result in an addition of 145 g of bone. It is difficult to predict the impact that this small additional mass might have on an adult hyena's ability to hunt and capture prey (although we suspect it would be minimal). We can, however, predict the effects that a solid sagittal crest would have on patterns of stress in the skull during biting.

Our quantitative results showed that, overall, the presence of a sinus actually increased the amount of stress in the skull during biting (i.e. in comparison to the filled model, the normal model exhibited substantially higher stresses in the cranial vault) (Fig. 5). The presence of the sinus also decreased the efficiency of transferring muscle force into bite force. The filled model was more efficient, requiring less muscle force to produce a bite force of 5500 N. FE analyses solve for static equilibrium in which input (muscle) forces are balanced by output (bite) forces and stress. Because there was overall less stress in the filled model, it follows that bite force was higher. This suggests that a filled arch-shaped crest would allow for the generation of higher bite forces than a sinus-filled crest, which might be advantageous for an animal that makes its living cracking open bones. However, we have observed extant spotted hyenas cracking open giraffe long bones up to 7 cm in diameter, so their pneumatized skulls allow them to cope effectively even with bones much larger than those of their usual prey. Furthermore, the filled model exhibited slightly higher stress concentrations in the facial region, which indicate 'weak spots' that are prone to failure under very high loads. The sinus therefore appears to reflect a trade-off between maximizing efficiency in force production and minimizing regions of stress concentration.

Although the normal model experienced more stress than the filled model, the qualitative comparisons indicate that the skull may be more evenly stressed in the normal model. This is particularly striking in light of the fact that the normal model required higher muscle forces to achieve the same bite force than the filled model. Therefore, even under larger loads, the normal model had areas of lower stress in the facial region than did the filled model.

For example, the areas of highly concentrated stress in the orbit and forehead of the filled model predict that the bone in these areas would reach the point of failure under lower muscle loads than the same areas in the normal model. This highlights the significant role played by the fronto-parietal sinus in moving forces away from the face, through the forehead to the cranial vault. Thus, there appears to be a unique complex comprised of the elongated fronto-parietal sinus and the vaulted forehead that is critical for stress dissipation in the skulls of these bone-cracking hyenas. When the sinus in the sagittal crest is absent, as in our filled model, the force transmission pathway from the face to the crest is disrupted at the transition from pneumatized to solid bone. A critical next step in understanding the biomechanical adaptations for durophagy would be to compare the arc of stress dissipation that we have demonstrated in hyaenids with that in a borophagine canid, which has similar vaulting in the forehead but lacks an elongated fronto-parietal sinus beneath the sagittal crest. We would expect to find a pattern similar to that in our filled model, lacking the advantages of an elongated fronto-parietal sinus to evenly dissipate stress away from the facial region.

ACKNOWLEDGEMENTS

We are grateful to the Kenyan Office of the President, the Narok County Council, the Senior Warden of the Masai Mara National Reserve, the National Museums of Kenya, and the Kenyan Wildlife Service for their permission to collect the specimen used in the present study, and for their cooperation and support. We also are indebted to Sean Werle and Ian Grosse for their help on this project, and to Kevin Berger and the Department of Radiology at MSU. We thank Joe Vorro, Tamara Reid-Bush, and Andy Farke for valuable conversations on this work. This research was funded by an IRGP grant from Michigan State University (S.T.S., K.E.H., B.L.L.), as well as NSF grants IOB 0618022 (K.E.H., B.L.L.) and IOB 0447616 (E.R.D.).

REFERENCES

- Biknevicius AR, Ruff CB. 1992.** The structure of the mandibular corpus and its relationship to feeding behaviours in extant carnivores. *Journal of Zoology* **228**: 479–507.
- Biknevicius AR, Van Valkenburgh B. 1996.** Design for killing: craniodental adaptations of predators. In: Gittleman JL, ed. *Carnivore behavior, ecology, and evolution*. Ithaca, NY: Cornell University Press, 393–428.
- Binder WJ, Van Valkenburgh B. 2000.** Development of bite strength and feeding behaviour in juvenile spotted hyenas (*Crocuta crocuta*). *Journal of Zoology* **252**: 273–283.

- Buckland-Wright JC. 1969.** Craniological observations on *Hyaena* and *Crocota* (Mammalia). *Journal of Zoology, London* **159**: 17–29.
- Buckland-Wright JC. 1971.** The distribution of biting forces in the skulls of dogs and cats. *Journal of Dental Research* **50**: 1168–1169.
- Buckland-Wright JC. 1978.** Bone structure and the patterns of force transmission in the cat skull (*Felis catus*). *Journal of Morphology* **155**: 35–62.
- Currey JD. 2002.** *Bones: structures and mechanics*. Princeton, NJ: Princeton University Press.
- Davis DD. 1964.** The giant panda: a morphological study of evolutionary mechanisms. *Fieldiana: Zoology Memoirs* **3**: 1–339.
- Dessem D. 1989.** Interaction between jaw-muscle recruitment and jaw-joint forces in *Canis familiaris*. *Journal of Anatomy* **164**: 101–121.
- Dumont ER, Piccirillo J, Grosse IR. 2005.** Finite-element analysis of biting behavior and bone stress in the facial skeletons of bats. *The Anatomical Record* **283**: 319–330.
- Erickson GM, Van Kirk SD, Su J, Levenston ME, Caler WE, Carter DR. 1996.** Bite-force estimation for *Tyrannosaurus rex* from tooth-marked bones. *Nature* **382**: 706–708.
- Frank LG, Holekamp KE, Smale L. 1995.** Dominance, demography, and reproductive success of female spotted hyenas. In: Sinclair ARE, Arcese P, eds. *Serengeti II: dynamics, management, and conservation of an ecosystem*. Chicago, IL: University of Chicago Press, 364–384.
- Gorniak GC, Gans C. 1980.** Quantitative assay of electromyograms during mastication in domestic cats (*Felis catus*). *Journal of Morphology* **163**: 253–281.
- Grosse IR, Dumont ER, Tolleson A, Coletta CE. 2007.** Techniques for modeling muscle-induced forces in finite element models of skeletal structures. *The Anatomical Record* **290**: 1069–1088.
- Hylander WL, Ravosa MJ, Ross C. 2004.** Jaw muscle recruitment patterns during mastication in anthropoids and prosimians. In: Anapol F, German RZ, Jablonski NG, eds. *Shaping primate evolution*. Cambridge: Cambridge University Press, 229–257.
- Jin C, Ciochon RL, Dong W, Hunt RMJ, Liu J, Jaeger M, Zhu Q. 2007.** The first skull of the earliest giant panda. *Proceedings of the National Academy of Sciences of the United States of America* **104**: 10932–10937.
- Joeckel RM. 1998.** Unique frontal sinuses in fossil and living Hyaenidae (Mammalia, Carnivora): description and interpretation. *Journal of Vertebrate Paleontology* **18**: 627–639.
- Koepfli KP, Jenks SM, Eizirik E, Zahirpour T, Van Valkenburgh B, Wayne RK. 2006.** Molecular systematics of the Hyaenidae: relationships of a relictual lineage resolved by molecular supermatrix. *Molecular Phylogenetics and Evolution* **38**: 603–620.
- Lewis ME, Werdelin L. 2000.** The evolution of spotted hyenas (*Crocota*). *IUCN Hyaena Specialist Group Newsletter* **7**: 34–36.
- Meers MB. 2002.** Maximum bite force and prey size of *Tyrannosaurus rex* and their relationships to the inference of feeding behavior. *Historical Biology* **16**: 1–12.
- Negus V. 1958.** *The comparative anatomy and physiology of the nose and paranasal sinuses*. Edinburgh: E&S Livingstone Ltd.
- Novocosky BJ, Popkin PRW. 2005.** Canidae volume bone mineral density values: an application to sites in western Canada. *Journal of Archaeological Science* **32**: 1677–1690.
- Paulli S. 1900.** Über die Pneumaticität des Schädels bei den Säugethieren. III. Über die Morphologie des Siebbeins und die der Pneumaticität bei den Insectivoren, Hyracoideen, Chiroptera, Carnivoren, Pinnipedien, Edentaten, Prosimiern und Primaten. *Morphologisches Jahrbuch* **28**: 483–564.
- Rensberger JM. 1999.** Enamel microstructural specialization in the canine of the spotted hyena (*Crocota crocuta*). *Scanning Microscopy* **13**: 343–361.
- Rensberger JM, Wang X. 2005.** Microstructural reinforcement in the canine enamel of the hyaenid *Crocota crocuta*, the felid *Puma concolor* and the Late Miocene Canid *Borophagus secundus*. *Journal of Mammalian Evolution* **12**: 379–403.
- Ross CF. 2005.** Finite element analysis in vertebrate biomechanics. *The Anatomical Record* **283A**: 253–258.
- Schweikher FP. 1930.** Ectocranial suture closure in the hyaenas. *American Journal of Anatomy* **45**: 443–460.
- Stefen C. 1997.** Differences in Hunter-Schreger bands of carnivores. In: Koenigswald WV, Sander PM, eds. *Tooth enamel microstructure*. Rotterdam: Balkema Press, 123–136.
- Strait DS, Wang Q, Dechow PC, Ross CF, Richmond BG, Spencer MA, Patel BA. 2005.** Modeling elastic properties in finite-element analysis: how much precision is needed to produce an accurate model? *The Anatomical Record* **283A**: 275–287.
- Therrien F. 2005.** Mandibular force profiles of extant carnivorans and implications for the feeding behaviour of extinct predators. *Journal of Zoology (London)* **267**: 249–270.
- Van Valkenburgh B. 2007.** Deja vu: the evolution of feeding morphologies in the Carnivora. *Integrative and Comparative Biology* **47**: 147–163.
- Verrue V, Dermaut L, Verheghe B. 2001.** Three-dimensional finite element modelling of a dog skull for the simulation of initial orthopaedic displacements. *European Journal of Orthodontics* **23**: 517–527.
- Wainwright PC, Reilly SM, eds. 1994.** *Ecological morphology*. Chicago, IL: University of Chicago Press.
- Wang Q, Strait DS, Dechow PC. 2006.** A comparison of cortical elastic properties in the craniofacial skeletons of three primate species and its relevance to the study of human evolution. *Journal of Human Evolution* **51**: 375–382.
- Werdelin L. 1989.** Constraint and adaptation in the bone-cracking canid *Osteoborus* (Mammalia: Canidae). *Paleobiology* **15**: 387–401.